Chemical Engineering Journal 172 (2011) 623–633

Contents lists available at ScienceDirect

Chemical Engineering Journal

journal homepage: www.elsevier.com/locate/cej

Kinetic modeling analysis for the removal of Cr(III) by Diphonix resin

Sandra Fernandes, Licínio M. Gando-Ferreira*

Centre of Chemical Processes Engineering and Forest Products (CIEQPF), Department of Chemical Engineering, University of Coimbra, Rua Sílvio Lima, 3030-790 Coimbra, Portugal

ARTICLE INFO

Article history:
Received 18 April 2011
Received in revised form 3 June 2011
Accepted 8 June 2011

Keywords:
Equilibrium and kinetics
Diphonix resin
Chromium and copper
Shrinking core model
Pore diffusion model

ABSTRACT

The sorption of Cr(III) and Cu(II) ions from aqueous solutions with the Diphonix resin in the sodium form have been investigated. Irreversible ion-exchange equilibrium isotherms were obtained for each pair metal/resin and well described by the Langmuir and Langmuir–Freundlich models. The maximum exchange capacities, which are temperature dependent, were estimated to be 2.73 and 3.74 meq/$g_{dryresin}$ for Cr(III) at 25 and 50 °C, respectively. For Cu(II), those values were 2.45 and 3.17 meq/$g_{dryresin}$. The effects of resin dosage, initial chromium concentration and initial pH on the uptake rate of Cr(III) were studied. The pseudo-second-order rate, pore diffusion and shrinking core models were applied for describing the kinetic data. The shrinking core model, based on non-steady state intraparticle diffusion, enabled a more realistic prediction of the evolution of concentrations of chromium and sodium in solution with time. By fitting the model equations to experimental data, the effective pore diffusivities of Cr(III), $D_{pef} = 2.66 \times 10^{-11}$ m^2/s for initial metal concentrations of 250 and 500 mg/L and, $D_{pef} = 5.31 \times 10^{-11}$ m^2/s for initial concentration of 750 mg/L were evaluated.

1. Introduction

There are a wide variety of industries such as electroplating, leather tanning, plastic manufacturing and metallurgical processes that generate large quantities of effluents with heavy metals. Heavy metals are important sources of environmental pollution, even in low concentration, because are non-degradable and thus persistent. The electroplating plants produce rinsed waters and wastewaters containing high concentrations of metals, especially chromium. This metal is usually considered very toxic for humans, animals and even plants, being the hexavalent form potentially carcinogenic when inhaled. The chromium can be recovered from the treatment of the wastewaters in order to be reused in the plating baths, being thus possible to improve the global process economy. In these systems, copper is an important contaminant metal that can accumulate over time in the bath solution and as a consequence the bath should be either discarded or purified to avoid the degradation of the plating process.

Ion-exchange processes have been frequently used as an effective technique for the treatment of industrial effluents containing heavy metals and for the recovery of valuable metals [1–8]. The chelating resins have been often employed as ion-exchange materials since their ligands can selectively bind to metallic ions through ionic and coordinating interactions. The resin tested is a polyfunctional chelating ion exchanger containing both sulfonic and phosphonic acid groups. Most of works reported in the literature focus the selective removal of metal ions by Diphonix resin in the H^+ form. Chiarizia and co-workers [9,10] demonstrated that the Diphonix resin has strong affinity for Cr(III), Fe(III) and Ni(III) in acidic solutions. Although the resin in the Na^+ form exhibits lower exchange capacity than in the H^+ form, the sodium form is more suitable for removal of metal ions from concentrated alkaline or alkaline earth solutions such is the case of electroplating effluents.

Suitable mathematical models to describe the equilibrium and kinetics of sorption of species on ion-exchange resins are necessary for predicting the dynamic behavior of continuous fixed-bed column systems. The main goal of this paper is to evaluate the sorption kinetics of Cr(III) on Diphonix resin in the Na^+ form using different models. The kinetic of sorption of metal ions on ion-exchange resins have been investigated in numerous studies during the past 15 years. Most of these studies describe the uptake rates based on models mainly used for data fitting, such as the first or second order kinetic models [11–16], which do not necessarily reflect the kinetic mechanisms of the sorption process. For systems, in which the metal is taken up through an irreversible reaction, the conversion of the resin proceeds with an outer fully converted "shell" and an inner core still in its initial state separated by a front that moves from the particle surface to the centre – shrinking core process or shell-progressive mechanism. The approach usually followed to describe the overall process

* Corresponding author. Tel.: +351 239 798700.
E-mail address: lferreira@eq.uc.pt (L.M. Gando-Ferreira).

1385-8947/$ – see front matter © 2011 Elsevier B.V. All rights reserved.
doi:10.1016/j.cej.2011.06.020

Nomenclature

C	solute concentration in the fluid phase (mg/L)
D	intraparticular diffusion coefficient (cm^2/s)
k_2	rate constant of pseudo-second-order model (g_{resin}/mg h)
K_L	isotherm parameter
m_p	particle mass (g)
m	isotherm parameter
q	adsorbed solute concentration in equilibrium with the liquid concentration (mg/g_{res})
q_t	amount adsorbed at time t (mg/g_{res})
q_m	maximum adsorption capacity of the adsorbent (mg/g)
r	radial position inside particles (cm)
r^*	normalized particle radial coordinate in the shrinking core model ($(r-R_f)/(R_0-R_f)$)
R	universal gas constant (kJ/mol K)
R_f	radial position of the reaction front (cm)
R_0	particle radius (cm)
T	temperature (K)
t	time (s)
u	normalized particle radial coordinate in the pore diffusion model
V_L	liquid volume (cm^3)
X	dimensionless solute concentration in the liquid phase (–)

Greek letters

$(-\Delta H)$	adsorption heat (kJ/mol)
ε_p	wet particle porosity
ζ	capacity factor ($m_p q_e/V_L C_0$)
ρ_h	wet density (g/cm^3)
τ_p	diffusion time constant (R_0/D_p^2)
θ	normalized time (t/τ_p)
ϕ	normalized radial position of the reaction front (R_f/R_0)

Subscripts

e	equilibrium
ef	effective
F	Freundlich
L	Langmuir
LF	Langmuir–Freundlich
0	initial
p	pore

considers the pseudo-steady-state (PSS) diffusion approximation [17–20]. Pritzker [20], for example, applied this assumption for describing the sorption of Cu(II) and Co(III) onto an iminodiacetate chelating resin involving two distinct reaction fronts. It was observed that the PSS approximation does not enable to correctly interpret the kinetic results at high counter-ions concentrations. In our work, a shrinking core model that takes into account non-steady state diffusion was applied to interpret the experimental kinetics data for different operating conditions. Moreover, the pseudo-second-order equation and pore diffusion model were also tested. In the equilibrium studies were determined equilibrium isotherms and investigated the effect of temperature and HNO_3 concentration on the sorption of Cr(III) and Cu(II) on Diphonix resin.

2. Modeling

2.1. Equilibrium models

Considering that the ion-exchange process between sodium and metal ions studied lead to isotherms highly favorable (irreversible isotherms), the ion-exchange equilibrium between the solid and liquid phases can be modeled by using common adsorption isotherms as follows:

$$\text{Langmuir isotherm} \quad q = \frac{q_{mL} K_L C}{1 + K_L C} \tag{1}$$

$$\text{Freundlich isotherm} \quad q = K_F C^{n_F} \tag{2}$$

$$\text{Langmuir–Freundlich isotherm} \quad q = \frac{q_{mLF} K_{LF} C^{n_{LF}}}{1 + K_{LF} C^{n_{LF}}} \tag{3}$$

where q is the amount of Cr(III) adsorbed in the resin (mg/g_{res}), C is the equilibrium concentration (mg/L), q_{mL} and K_L are the Langmuir parameters, K_F and n_F the Freundlich parameters and q_{mLF}, K_{LF} and n_{LF} the Langmuir–Freundlich parameters.

2.2. Kinetic models

The kinetics of ion-exchange between solutes and an adsorbent is generally governed by two mass-transfer mechanisms: convective transport outside the particle and intraparticle diffusion. Further, intraparticle diffusion may occur either by diffusion through macropores, or through the gel structure of the resin, or through both steps. Several models have been used to describe the kinetics of metallic species sorption into resins, being the most popular the first order model and pseudo second-order model [11,12]. In this work, a first approach to model the kinetic data was based on the pseudo-second order rate expression in the form:

$$\frac{dq_t}{dt} = k_2 (q_e - q_t)^2 \tag{4}$$

where k_2 is the rate constant of pseudo-second order adsorption, q_e is the amount adsorbed under equilibrium conditions, and q_t is the amount adsorbed at time t.

Integrating Eq. (4) with the conditions $q_t = 0$ when $t = 0$ and $q_t = q_t$ when $t = t$, gives:

$$\frac{1}{q_e - q_t} = \frac{1}{q_e} + k_2 t \tag{5}$$

Re-arranging Eq. (5) results the expression

$$\frac{t}{q_t} = \frac{1}{k_2 q_e^2} + \frac{t}{q_e} \tag{6}$$

In addition, the pore diffusion and shrinking core models were also applied in order to better interpret the experimental kinetic results. In both models, it was assumed that: (i) intraparticle mass transfer takes place by diffusion inside pores; (ii) the process is isothermal; (iii) the film mass transfer resistance is negligible and (iv) the resin particles are spherical with uniform size and density. In the case of pore diffusion model, the following dimensionless mass balance equation incorporating the Langmuir isotherm for describing the instantaneous equilibrium at the pore/wall interface with respective initial and boundary conditions, may be written for the species Cr(III):

Mass balance for the resin particle

$$\frac{\partial X_p(u,\theta)}{\partial \theta} = \frac{\varepsilon_p}{\varepsilon_p + (K_L q_{mL} \rho_h / (1 + K_L C_o X_p)^2)} \left\{ \left(\frac{2}{u} \right) \frac{\partial X_p(u,\theta)}{\partial u} + \frac{\partial^2 X_p(u,\theta)}{\partial u^2} \right\} \tag{7}$$

Mass balance in the bulk phase

$$\frac{\partial X(\theta)}{\partial \theta} = -3\varepsilon_p \zeta \frac{1 + K_L C_0}{K_L q_{mL} \rho_h} \frac{\partial X_p(u,\theta)}{\partial u}\bigg|_{u=1} \tag{8}$$

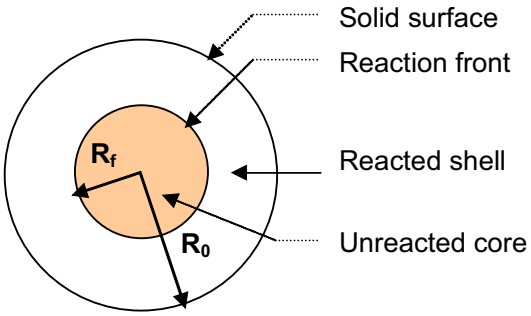

Fig. 1. Schematic representation of the shrinking core model.

Boundary conditions

- symmetry condition ($u=0$)

$$\left.\frac{\partial X_p(u,\theta)}{\partial u}\right|_{u=1} = 0 \tag{9}$$

- interface pore/external solution ($u=1$)

$$X_p(1,\theta) = X(\theta) \tag{10}$$

Initial condition

$$X_p(u,0) = 0 \quad \text{for} \quad u < 1 \quad \text{and} \quad X_p(u,0) = 1 \quad \text{for} \quad u = 1 \tag{11}$$

In the above equations, $X = C/C_0$ and $X_p = C_p/C_0$ are the dimensionless concentrations of Cr(III) in the bulk liquid phase and in the liquid inside particle pores, respectively; ε_p is the particle porosity and ρ_h wet resin density; $\theta = t/\tau_p$ is the normalized time, where $\tau_p = R_0^2/D_p$ is the diffusion time constant, being R_0 the particle radius and D_p pore diffusivity coefficient; $u = r/R_0$ is the normalized particle radial coordinate. The only dimensionless group of the model is the capacity parameter, ζ, defined as:

$$\zeta = \frac{m_p}{V_L}\frac{q_e}{C_0} \tag{12}$$

where m_p is the particle mass, q_e is solute concentration in equilibrium with C_0 and V_L is liquid volume. Numerical integration of Eqs. (7)–(11) was achieved using PDECOL package [21].

The shrinking core model considers a reaction front which moves from the surface to the centre of the particle as shown in Fig. 1 and takes into account the following hypothesis: (i) the transport of species inside the resin occurs only by diffusion; (ii) reaction between chromium and sodium is instantaneous and irreversible; (iii) evolution of the reaction front is controlled by Cr(III) that releases Na^+ from the resin and (iv) the mass transport of species beyond the front is negligible, therefore, the unreacted core remains in the original form.

The mass balance inside the particle for species i is given by:

$$\varepsilon_p \frac{\partial C_{p_i}(r,t)}{\partial t} = \frac{1}{r^2}\frac{\partial}{\partial r}\left\{r^2 \varepsilon_p D_{p_i}\frac{\partial C_{p_i}(r,t)}{\partial r}\right\}, \quad i = 1 \text{ (Cr) and } 2 \text{ (Na)}, \quad R_f < r \le R_0 \tag{13}$$

The equation for the reaction front is,

$$-\varepsilon_p D_{p_1}\left.\frac{\partial C_{p_1}(r,t)}{\partial r}\right|_{r=R_f} = \rho_h q_1 \frac{dR_f}{dt} \tag{14}$$

The mass balance in the bulk phase for species i leads to:

$$-V_L\frac{dC_i}{dt} = m_p\rho_h\varepsilon_p\frac{d\overline{C}_{p_i}}{dt} + \gamma_i\frac{3m_p{R_f}^2 q_1}{{R_0}^3}\frac{dR_f}{dt} \tag{15}$$

where R_f is the position of the "moving front", q_1 is ion-exchange capacity of species 1 obtained from the equilibrium isotherm, $\gamma_1 = -1$ for Cr and $\gamma_2 = \alpha$ for Na (α is the fraction of species 2 reacted).

The time derivative of the average pore concentration for species i is evaluated as,

$$\frac{d\overline{C}_{p_i}}{dt} = \frac{3}{R_0^3}\frac{d}{dt}\int_{R_f}^{R_0} r^2 C_{p_i} dt \tag{16}$$

The left member of Eq. (16) can be integrated using Eq. (13) resulting in

$$\frac{d\overline{C}_{p_i}}{dt} = -\frac{3}{R_0^3}R_f^2 C_{p_i}\Big|_{r=R_f}\frac{dR_f}{dt} + \frac{3}{R_0^3}\left[R_0^2 D_{p_i}\left.\frac{\partial C_{p_i}(r,t)}{\partial r}\right|_{r=R_0} - R_f^2 D_{p_i}\left.\frac{\partial C_{p_i}(r,t)}{\partial r}\right|_{r=R_f}\right] \tag{17}$$

The boundary and initial conditions are as follows:

$$r = R_f, \quad C_{p_1}(R_f,t) = 0 \tag{18}$$

$$C_{p_2}(R_f,t) = \frac{\alpha m_p(1 - R_f^3/R_0^3)q_1}{V_L} \tag{19}$$

$$r = R_0, \quad C_{p_i}(R_0,t) = C_i(t) \tag{20}$$

$$t = 0, \quad C_{p_i}(r,0) = 0; \quad C_1(0) = C_{1_0}; \quad C_2(0) = 0 \text{ and } R_f = R_0 \tag{21}$$

Introducing in Eqs. (13)–(21) the following normalized variables:

$$X_1 = \frac{C_1}{C_{1_0}}, \quad X_2 = \frac{C_2}{C_{1_0}}, \quad X_{p_1} = \frac{C_{p_1}}{C_{1_0}}, \quad X_{p_2} = \frac{C_{p_2}}{C_{1_0}}, \quad \phi = \frac{R_f}{R_0},$$

$$r^* = \frac{r - R_f}{R_0 - R_f}, \quad \theta = \frac{t}{\tau_p}\left(\tau_p = \frac{R_0^2}{D_{p_1}}\right), \quad \zeta = \frac{m_p}{V_L}\frac{q_1}{C_{1_0}}$$

and after making the appropriate substitutions we get:

Mass balance inside the particles for species i

$$\frac{\partial X_{p_i}(r^*,\theta)}{\partial\theta} = \beta_i\left\{\frac{2}{(1-\phi)[\phi + r^*(1-\phi)]} - \left[\frac{(1-\phi)r^* + \phi - 1}{(1-\phi)^2}\right]\frac{\partial\phi}{\partial\theta}\right\}\frac{\partial X_{p_i}(r^*,\theta)}{\partial r^*} + \beta_i\left[\frac{1}{(1-\phi)^2}\frac{\partial^2 X_{p_i}(r^*,\theta)}{\partial r^{*2}}\right] \tag{22}$$

where $\beta_1 = 1$ for Cr and $\beta_2 = D_{p_2}/D_{p_1}$ for Na.

It should be noted that to convert the term of the derivative of concentration with respect to time as function of the new normalized variable r^*, in Eq. (22), we considered the variable r^* depending on both variables r and $R_f(t)$.

Equation for the reaction front

$$\frac{d\phi}{d\theta} = -\frac{\varepsilon_p C_{1_0}}{(1-\phi)\rho_h q_1}\left.\frac{\partial X_{p_1}(r^*,\theta)}{\partial r^*}\right|_{r^*=0} \tag{23}$$

Mass balance in the bulk phase for species i

$$\frac{dX_i(\theta)}{d\theta} = \frac{3\varepsilon_p C_{1_0}\zeta}{\rho_h q_1}\frac{1}{(1-\phi)}\beta_i\left(\phi^2\left.\frac{\partial X_{p_i}(r^*,\theta)}{\partial r^*}\right|_{r^*=0} - \left.\frac{\partial X_{p_i}(r^*,\theta)}{\partial r^*}\right|_{r^*=1}\right) + \frac{d\phi}{d\theta}\phi^2\left(\frac{3\varepsilon_p C_{1_0}\zeta}{\rho_h q_1}X_{p_i}\Big|_{r^*=0} - \gamma_i 3\zeta\right) \tag{24}$$

Table 1
Characteristic parameters of Diphonix resin.

Polymer structure	Polystyrene/divinylbenzene
Functional group	Diphosphonic and sulphonic acid
Physical form	Spherical beads
Efective size (mm)	0.15–0.3
Wet density, ρ_h (g/cm^3)	0.94
Moisture content (%)	58.3
Wet particle porosity, ε_p	0.70
Capacity (meq/g)	3.03

Boundary and initial conditions

$$r^* = 0, \quad X_{p_1}(0,\theta) = 0 \tag{25}$$

$$X_{p_2}(0,\theta) = \frac{\alpha m_p (1-\phi^3) q_1}{C_{1_0} V_L} \tag{26}$$

$$r^* = 1, \quad X_{p_i}(1,\theta) = X_i(\theta) \tag{27}$$

$$\theta = 0, \quad X_{p_i}(r^*,0) = 0; \quad X_1(0) = 1; \quad X_2(0) = 0 \quad \text{and} \quad \phi = 1 \tag{28}$$

Numerical solutions of Eqs. (22)–(28) were performed by discretizing Eq. (22) in N interior points using global orthogonal collocation with Lagrange polynomials as basis functions [22]. The final system of 2^*N+3 ordinary differential equations was numerically integrated with LSODE package [23].

3. Experimental

3.1. Materials

The resin Diphonix (EIChrom) was used in this study, and their chemical and physical characteristics are shown in Table 1. All the chemicals used were of analytical grade and obtained from Ridel-de-Haën.

3.2. Equilibrium and kinetic experiments

Before the experiments, three consecutive elution-washing cycles using 2 M HCl, H_2O and 2 M NaOH were applied to resin in order to remove solvents and other preparation chemicals. The last step of the conditioning consisted in percolating an excess of NaOH through the column in order to convert the resin to sodium form. The excess of OH^- or Cl^- ions was removed from the resin by rinsing with deionized water until the pH of the eluent was 6–7.

The synthetic solutions of chromium and copper were prepared by dissolving appropriate amounts of $Cr(NO_3)_3{\cdot}9H_2O$ and $Cu(NO_3)_2{\cdot}2.5H_2O$ in deionized water. The uptake of chromium and copper by the resins was studied in batch mode. In the case of equilibrium experiments, 40 mL of a synthetic solution at different initial concentrations were added into a flask with 1 g of pre-conditioned resin. The flasks were sealed and kept at constant temperature (25 or 50 °C) in a shaker for 24 h. For studying the effect of nitric acid, the chromium and copper salts were prepared in the presence of different concentrations of HNO_3. The data of this study were obtained after 9 days of equilibration.

The resins were separated by vacuum filtration using a Buchner funnel and a filter with a porosity of 0.45 μm. Some aliquots of liquid were analyzed in order to determine the concentration of metals and solution pH. The concentrations of sodium ion, total chromium and copper ion were quantified by Flame Atomic Absorption Spectrophotometry (FAAS), Perkin Elmer 3300. The pH measurement was carried out potentiometrically using a WTW pH meter, model Inolab level.

The kinetic experiments were performed with initial concentrations of chromium corresponding to 250, 500 and 750 mg/L while maintaining the resin mass constant (0.5 g). For initial pH effect, 500 mg/L of Cr(III) and 0.5 g of resin were utilized and the pH was adjusted to the desired value by drop wise 0.1 M HNO_3. To study the resin dosage effect, different dosages (0.5, 0.75 and 1 g) were added to solution with 500 mg/L of Cr(III). The solutions were kept under agitation at 25 °C. Small resin free samples were withdrawn periodically using a pipette and analyzed as described above.

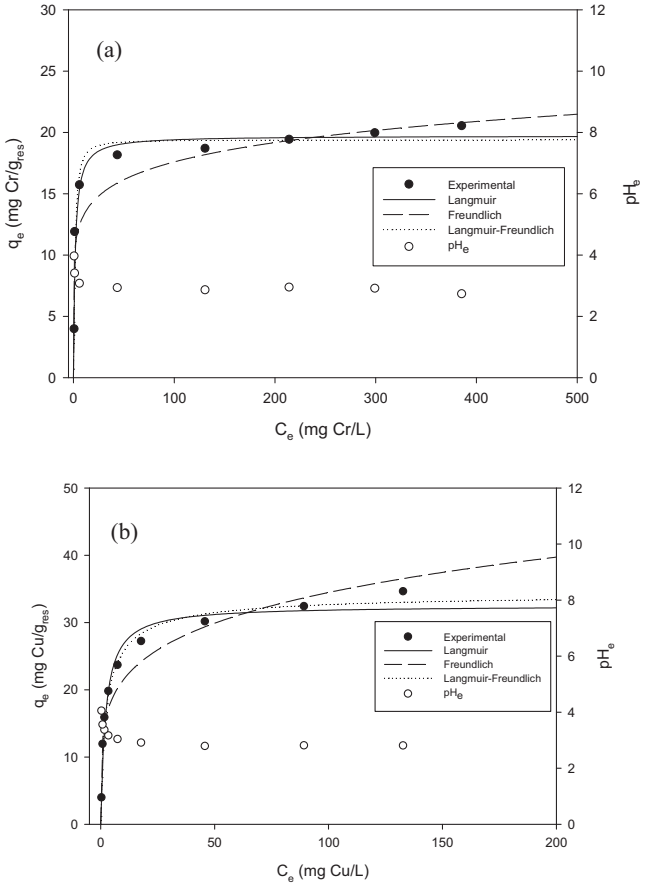

Fig. 2. Equilibrium sorption isotherms for metal ion on Diphonix ((a) – Cr(III); (b) – Cu(II)) and final pH values. The symbols represent experimental data whereas lines are the best fitting of data by Langmuir, Freundlich and Langmuir–Freundlich models.

4. Results and discussion

4.1. Equilibrium studies

Experimental and calculated data of ion-exchange equilibrium for uptake of Cr(III) and Cu(II) by Diphonix resin are shown in Fig. 2(a) and (b). The shape of the curves indicates that the sorption of both metals by the resin is highly favorable, thus can be considered quasi-irreversible ion-exchange isotherms. The equilibrium models, Eqs. (1)–(3), were fitted to the experimental data and the parameters were estimated by using a non-linear optimization routine, GREG software [24]. The parameter values for each model tested are summarized in Table 2. According to sum of the square errors (SS), the best fitting was achieved with the Langmuir–Freundlich model for the exchange systems Cr(III)/Na and Cu(II)/Na. However, for Cr(III) sorption the Langmuir model was considered instead of Langmuir–Freundlich model, since the n_{LF} value do not have physical meaning in this case. The exchange capacity of the resin for chromium (2.73 meq/$g_{dryresin}$) was estimated to be a little higher than the capacity for copper, i.e. 2.45 meq/$g_{dryresin.}$ A higher capacity of 3.4 meq/$g_{dryresin}$ for Cr(III) using other commercial lot of Diphonix resin was found by the

Table 2
Isotherm parameters for sorption of Cr(III) and Cu(II) on Diphonix resin.

Metal	Langmuir			Freundlich			Langmuir–Freundlich			
	q_{mL} (mg/g_{res})	K_L (L/mg)	SS	K_F (L/g_{res})	n_F	SS	q_{mLF} (mg/g_{res})	K_{LF} (L/g_{res})	n_{LF}	SS
Cr(III)	19.73 2.73[a]	0.59	19.6	9.94	0.12	55.6	19.40 2.68[a]	0.54	1.36	18.1
Cu(II)	32.52 2.45[a]	0.47	23.0	13.41	0.21	88.5	34.46 2.60[a]	0.48	0.79	17.1

[a] meq/$g_{dryresin}$.

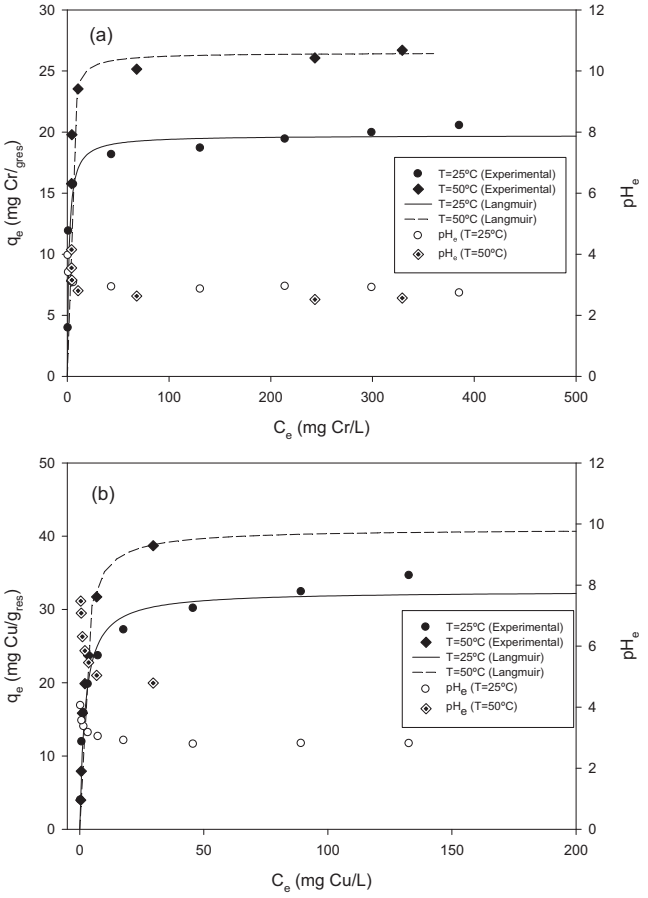

Fig. 3. Equilibrium sorption isotherms for metal ion on Diphonix ((a) – Cr(III); (b) – Cu(II)) and final pH values at two different temperatures. The symbols represent experimental data whereas lines are the best fitting of data by Langmuir model.

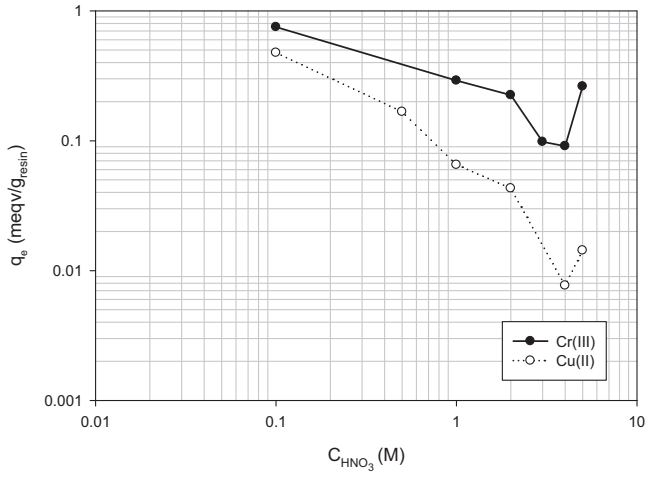

Fig. 4. Effect of acid nitric concentration on the uptake of Cr(III) and Cu(II) by the Diphonix resin.

same authors [25]. The equilibrium pH values, varying in the range 2.8–4.0, as function of metal concentration in solution can also be seen in Fig. 2. The metal uptake by the resin leads to a decrease of the solution pH, i.e. $\Delta pH = pH_{final} - pH_{initial} < 0$. This suggests that the two functional groups of the resin (sulfonic and *gem*-diphosphonic acid groups) were not completely converted to sodium form, thus it is expectable to occur some exchange between H^+ ions bounded to resin and metallic ions of the solution.

In the pH range of 3–4, it was observed that the uptake of 1 mol of Cr(III) by the resin releases approximately 2.7 mol of Na^+ while the uptake of 1 mol of Cu(II) is exchanged with around 1.8 mol of Na^+. Therefore, one can conclude that most of chromium and copper exchanged with the resin are in the form Cr^{3+} and Cu^{2+}, respectively. It is worth mentioning that Cr(III) forms different species in aqueous solution depending on the pH and redox potential. The redox potential measured in all the solutions was approximately of 400 mV. For this potential, at pH = 3, the predominant species are Cr^{3+} (84.4%) and $Cr(OH)^{2+}$ (14.7%) while at pH = 4.0 the species predominant are Cr^{3+} (30.8%), $Cr(OH)^{2+}$ (57.1%) and $Cr_2(OH)_2{}^{4+}$ (11%) [26].

Fig. 3 shows the effect of temperature on the sorption of metal ion onto Diphonix resin. According to Figure, the ion-exchange capacity is increased with increasing temperature. This may be explained by the formation of more stable chelate complex between the metal and diphosphonic acid group of the resin at high temperatures. Some empirical studies show that the chelation reaction is affected by the temperature mainly due to entropy change during the sorption process [27]. The Langmuir model, previously indicated in Eq. (1), in which K_L constant is related to the temperature by $K_L = K_{L_0} \exp(-\Delta H/RT)$ fits well the experimental data. The parameter values estimated at temperatures of 25 and 50 °C are listed in Table 3. Increments of 1.01 and 0.72 meq/$g_{dryresin}$ in the sorption capacities of Cr(III) and Cu(II), respectively, were observed when the temperature varied from 25 to 50 °C. Considering the heat of adsorptions (ΔH) estimated for chromium (5.48 kJ/mol) and copper (8.35 kJ/mol), one can conclude that the sorption of metals on Diphonix resin is an endothermic process, then will be favored as the temperature increases.

The effect of initial HNO_3 concentration was also studied, and the equilibrium data are represented in Fig. 4. These data show that the exchange capacity of the resin is strongly dependent on the acid concentration. Indeed, the uptake of Cr(III) and Cu(II) decreases with the increase of acid concentration until 3–4 M HNO_3, and then increases. This result confirms the studies reported by Chiarizia et al. [9]. In Fig. 4, it is also evident that greater differences between the exchange capacities of the resin for both metals at higher acidities of the solution. For 0.1 M HNO_3, the sorption capacity of Cr(III) is 1.6 times higher than the capacity of Cu(II) whereas for 4 M HNO_3 that factor is of 11.8. Therefore, the differences in the affinity of resin by the two metals may be predetermined as function of nitric acid concentration. The acid dependency of the sorption data is due to the competition between metal and hydrogen ions for the binding

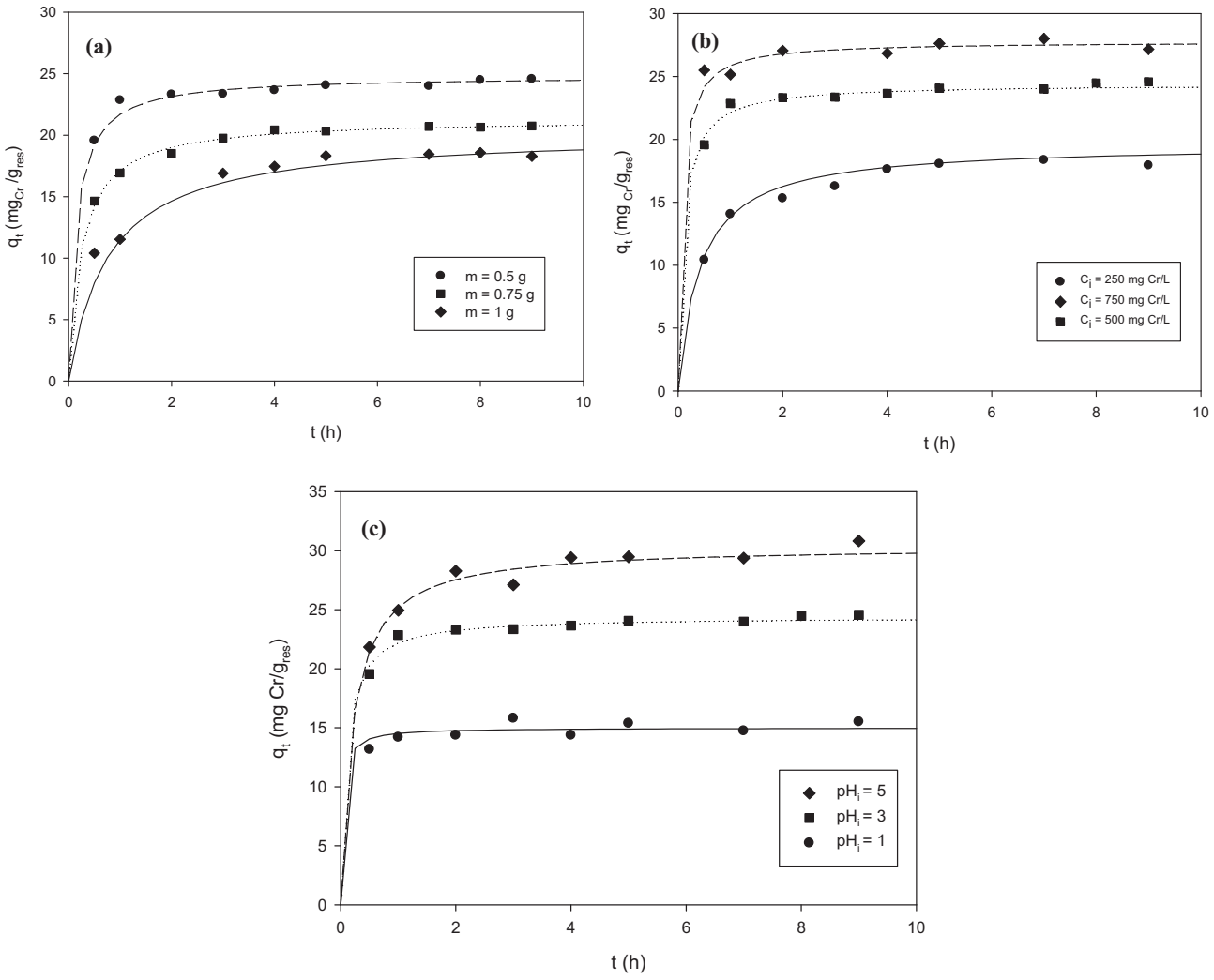

Fig. 5. Effect of resin dosage (a), initial concentration (b) and initial pH (c) on the rate of sorption of Cr(III) onto Diphonix resin. The symbols represent experimental data whereas lines are the best fitting of data by pseudo-second-order model.

sites of the resin. The resin acts through a dual mechanism in which a hydrophilic sulfonic acid group allows the access of non-specific ions into the polymeric network and a diphosphonic acid group is responsible by the formation of chelates with specific metal ions. Diphonix exhibits high affinity for polyvalent cations from moderately acidic solutions and its exchange capacity decreases with the increasing acidity of solution because the diphosphonate group in the resin becomes more protonated [9].

4.2. Kinetic studies

Fig. 5 shows kinetic results plotted as sorption rates of Cr(III) as function of contact time at different operating conditions (resin dosage, initial solute concentration and initial solution pH). The shape of the curves indicates that ion-exchange process is quite fast occurring 63–93% of the ultimate adsorbed value during the first hour of contact.

Regarding the effect of the resin dosage, the results illustrated in Fig. 5(a) show that when the resin concentration increases the amount exchanged per unit mass of resin, q_t, decreases, however, the percentage of removal of Cr(III) increases. The decrease of q_t can be attributed to the fact of some active sites of the resin remain unsaturated during the ion-exchange process. The change of resin dosage from 0.5 to 1.0 g causes an increment of removal of Cr(III) from 61.89 to 91.92%, under equilibrium conditions. The effect of initial concentration of chromium on q_t is shown in Fig. 5(b). The amount taken up by the resin increases with the increase in the initial Cr(III) concentration, however, the percentage of solute removed decreases. The percentage of chromium removed decreased from 90.75 to 45.78% when the initial concentration was varied from 250 to 750 mg/L. The effect of initial pH on q_t is shown

Table 3
Isotherm parameters for sorption of Cr(III) and Cu(II) on Diphonix resin at two different temperatures.

Metal	Temperature (°C)	q_{mL} (mg/g_{res})	q_{mL} (meq/g_{dryres})	K_L (L/mg)	K_{L_0} (L/mg)	ΔH (kJ/mol)
Cr(III)	25	19.73	2.73	0.59	5.37	5.48
	50	26.50	3.67	0.70		
Cu(II)	25	32.52	2.45	0.47	13.67	8.35
	50	41.00	3.10	0.61		

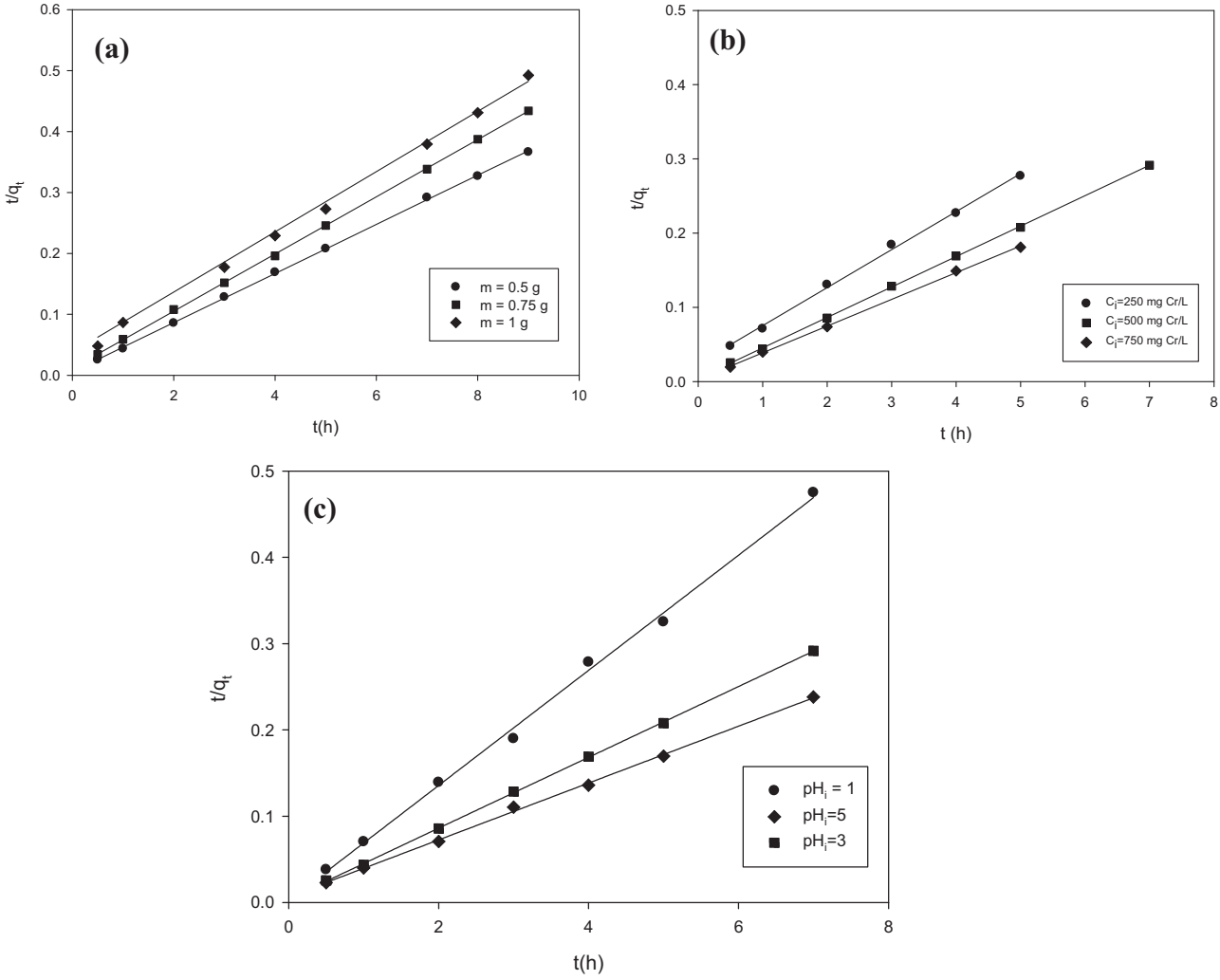

Fig. 6. Pseudo-second-order kinetics plots for the sorption of Cr(III) onto Diphonix resin: (a) – effect of dosage resin; (b) – effect of initial concentration and (c) – effect of initial pH.

in Fig. 5(c). The pH plays an important role in the exchange process between the ion-exchange resins and metal ions. Greater exchange capacity for Cr(III) was achieved at high initial pH of the solution as shown in Fig. 5(c), probably due to the reduced proton competition to Cr(III) binding with the functional groups of the resin. In this study, the percentage of chromium removed increased from 38.94 to 77.16% when the initial pH was varied from 1 to 5.

A first approach for interpreting the kinetic data was based on the pseudo-second-order kinetic model in its linearized form, Eq. (6). Using this equation, t/q_t was plotted against t for all the experiments (Fig. 6). The values of the parameters, q_e and k_2, estimated by fitting the model to the experimental data are presented in Table 4. The values of k_2 were found to decrease with increasing the resin dosage and initial pH, and with the decreasing the initial Cr(III) concentration. In Table 4 are also indicated h $(= k_2 q_e^2)$ values, where h can be regarded as the initial sorption rate as $q_t/t \to \infty$, and correlation coefficients (R^2). The increase in the values of h can be attributed to an increase in the driving force for mass transfer enabling that the solute molecules reach the surface of the resin particles in a shorter period of time. Good fittings were obtained using this model, being the R^2 values superior to 0.99 in all the cases. The comparison between the experimental and calculated q_t values can be seen in Fig. 5.

The second-order model does not enable to realistically describe the intraparticular transport of the solute and evaluate the effective intraparticular diffusion coefficient. Therefore, the kinetic data were further analyzed with the pore diffusion model (PDM) and shrinking core model (SCM). Simulated and experimental results of the concentration of solute(s) in external solution as function of time can be seen in Figs. 7–9. The operating conditions for all the experiments are indicated in Table 5. To evaluate the capacity parameter, ζ, exchange capacities for Cr(III) obtained

Table 4
Pseudo-second-order kinetic parameters for the sorption of Cr(III) on Diphonix resin.

Resin dosage	k_2 (g_{resin}/mg h)	q_e (mg/g_{resin})	$k_2 q_e^2$ (mg/g_{resin} h)	R^2
0.5	0.28	24.81	172.35	0.9997
0.75	0.19	21.32	86.36	0.9999
1.0	0.065	20.24	26.63	0.9891
Initial Cr(III) concentration	k_2 (g/mg h)	q_e (mg/g_{resin})		R^2
250	0.12	19.61	46.15	0.9976
500	0.40	24.39	237.95	0.9999
750	0.49	27.78	378.15	0.9994
Initial pH	k_2 (g/mg h)	q_e (mg/g_{resin})		R^2
1	2.02	14.99	453.89	0.9988
3	0.41	24.39	237.95	0.9971
5	0.16	30.40	378.15	0.9999

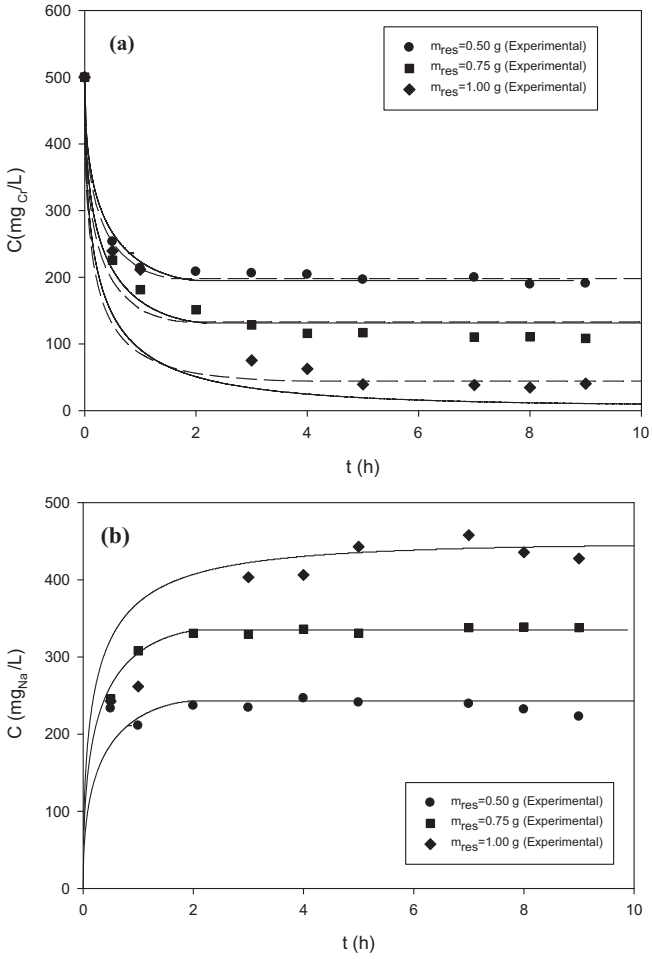

Fig. 7. Evolution of chromium (a) and sodium (b) concentrations in solution, for different resin dosages, during the sorption of Cr(III) into Diphonix resin. The symbols represent experimental data whereas the lines are the best fittings of shrinking core model (solid lines) and pore diffusion model (dot lines).

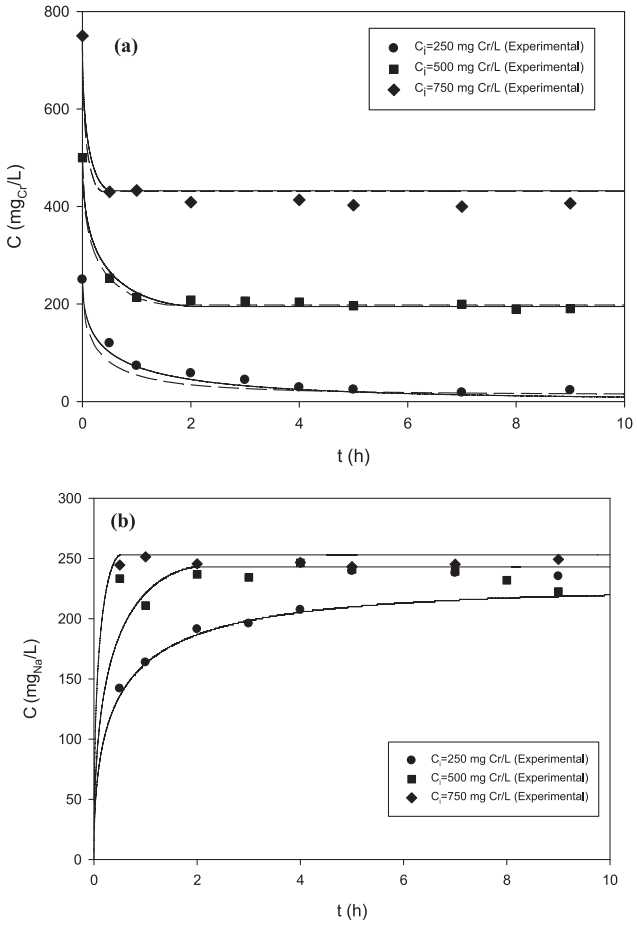

Fig. 8. Evolution of chromium (a) and sodium (b) concentrations in solution, for different initial Cr(III) concentrations, during the sorption of Cr(III) into Diphonix resin. The symbols represent experimental data whereas the lines are the best fittings of shrinking core model (solid lines) and pore diffusion model (dot lines).

from the equilibrium isotherms were used. For runs 1 and 5, a different lot of Diphonix resin was utilized with sorption capacity of 24.4 mg/g_{resin} (3.4 $meq/g_{dryresin}$) [25]. The ζ values for runs 2–4 were calculated considering q_1 = 19.7 mg/g_{resin} (Table 2). For runs 6 and 7, the exchange capacities of 15.0 and 30.4 mg/g_{resin} estimated from the pseudo-second-order model were considered.

Fig. 7 shows the evolution of concentration of Cr(III) and Na^+ with time at different resin dosages. It can be seen that when the resin dosage increases the ultimate concentration (equilibrium concentration) of Cr(III) decreases. Thus, this result is consistent with the increasing in the percentage of chromium removed as previously discussed. Contrarily, the Na^+ concentration increases as shown in Fig. 7(b), since the solution under equilibrium conditions is less concentrated in chromium implying that higher exchange with sodium ion occurred. In the case of evolution of Cr(III) concentration along time, both models describe reasonably well the transient period characterized by a fast kinetics, however, in the final stage the PDM predicts better the ultimate concentration, mainly for a resin dosage of 1.0 g. It should be noted that this

Table 5
Operating conditions for kinetic experiments.

Run	Resin dosage (g)	Initial Cr(III) concentration (mg/L)	Initial pH	ζ
1	0.5	500	3.3	0.61
2	0.75	500	3.3	0.74
3	1.0	500	3.3	0.99
4	0.5	250	3.4	0.99
5	0.5	750	3.1	0.41
6	0.5	500	1.5	0.38
7	0.5	500	5.0	0.78

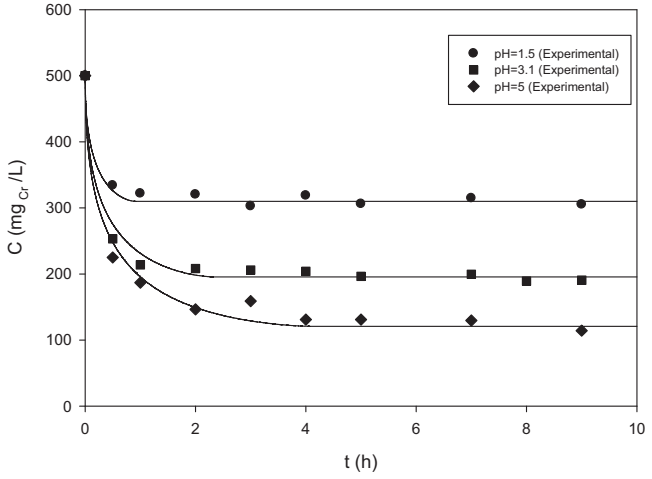

Fig. 9. Evolution of chromium concentration in solution, for different initial pH values, during the sorption of Cr(III) onto Diphonix resin. The symbols represent experimental data whereas the lines are the best fittings of shrinking core model.

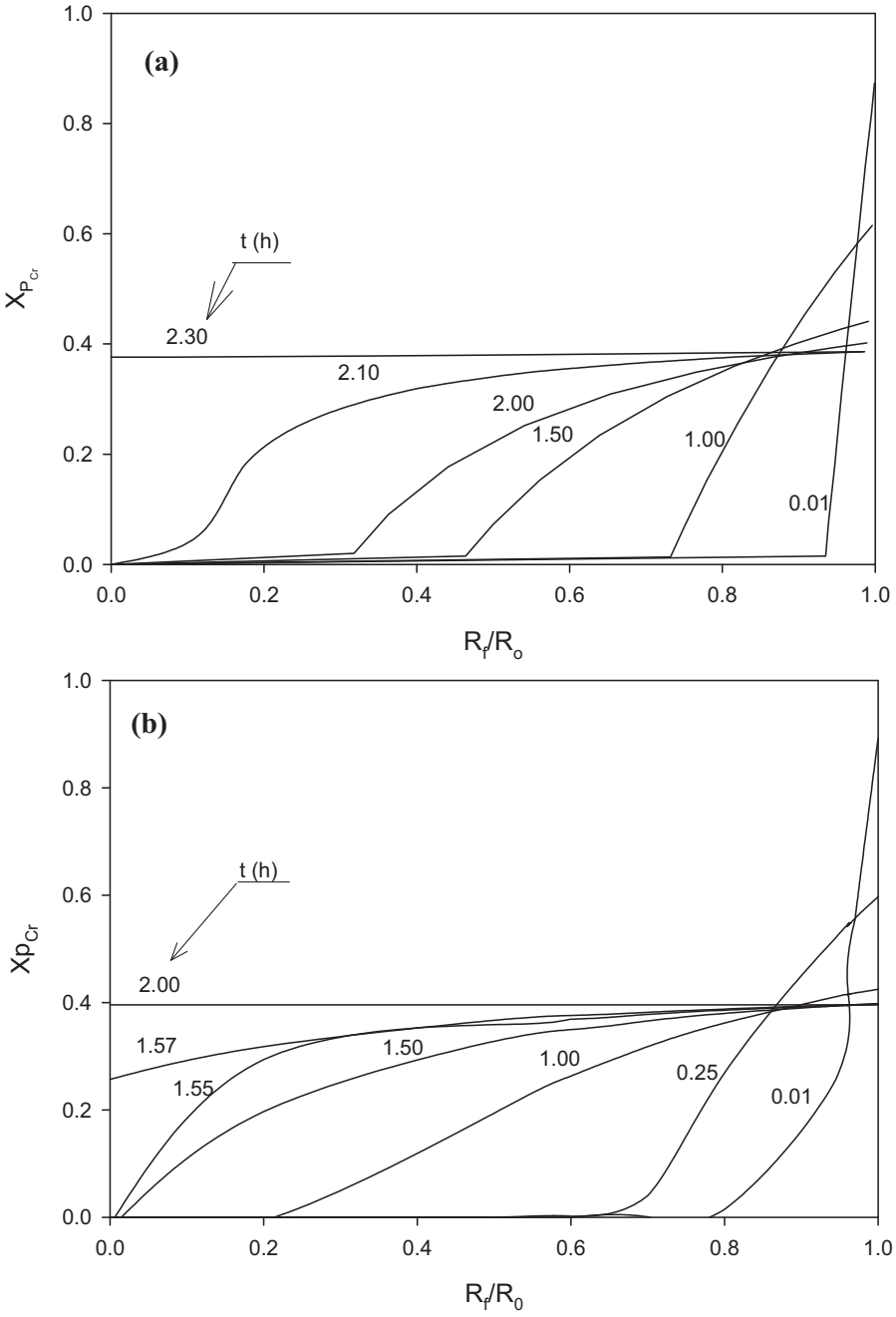

Fig. 10. Particle radial concentration profiles predicted by the shrinking core model (a) and pore diffusion model (b).

model only enables the description of the dynamic behavior of the Cr(III) species. The concentration change of sodium ion in solution as function of time is shown in Fig. 7(b). The data were predicted by the SCM using a fraction of sodium reacted α of 0.8 for runs 1 and 5 and, α of 0.9 for runs 2–4. The justification for the α values used in the simulations is based on the assumption of 80–90% of sodium bounded to resin is probably exchanged with trivalent chromium in the form Cr^{3+} as aforementioned in Section 4.1. The effective pore diffusivity coefficients $(\varepsilon_p D_p)$ estimated by fitting the models to experimental data are: $D_{pef(Cr)} = 2.66 \times 10^{-11}$ m^2/s and $D_{pef(Na)} = 5.22 \times 10^{-11}$ m^2/s.

Fig. 8 illustrates the evolution in time of the concentration profiles for Cr(III) and Na^+ under different initial chromium concentrations in solution. Obviously, when the initial chromium ion concentration is reduced the equilibrium concentration for both species decreases and thus leads to lower sorption capacities. The experimental results are well predicted by the pore diffusion and shrinking core models. For initial Cr(III) concentrations of 250 and 500 mg/L, the effective pore diffusivity coefficients calculated are ones previously indicated. For initial Cr(III) concentration of 750 mg/L, the values are: $D_{pef(Cr)} = 5.31 \times 10^{-11}$ m^2/s and $D_{pef(Na)} = 1.04 \times 10^{-10}$ m^2/s. This suggests that at high initial concentrations the kinetic nature of the process is changed as expected. For these conditions, there is a more pronounced decrease of solute concentration in the first 30 min (Fig. 8(a)) since the ions exhibit higher mobility, confirming thus the increasing in the values of pore diffusivity coefficients for both ions. The diffusivity value found for chromium is similar to those obtained from breakthrough curves by Cavaco et al. [25]. Fig. 9 shows concentration profiles of Cr(III) under different initial pH values. From the Figure, it can be observed

that this variable does not affect the kinetics process but determines the equilibrium concentration. At higher pH solution occurs an increase in the sorption capacity of Cr(III) and consequently a decrease in the ultimate concentration when the system achieves equilibrium conditions. There is a good agreement between experimental and calculated data using the SCM. The PDM was not applied because the equilibrium isotherms at initial pH of 1.5 and 5.0 were not determined experimentally.

The solution of the models (PDM and SCM) enables to predict concentration profiles for the species inside the resin pores during the sorption process. The radial profiles of Cr(III) at different times, for run 1, are illustrated in Fig. 10(a) and (b). It can be verified that qualitatively similar profiles are obtained from both models. However, in the first instant of the exchange process the profiles predicted by the SCM are much steeper and move more slowly than ones predicted by the other model. This behavior is more concordant with the irreversible character of the equilibrium isotherm. In addition, it is worth mentioning that the reaction front achieves the particle centre at $t = 2.1$ h according to the shrinking core model, and then the resin becomes quickly saturated (Fig. 10(a)).

The PDM and SCM, based on the particle diffusion as controlling mechanism, were able to describe the sorption kinetics for the removal of Cr(III) by Diphonix resin. This resin was recently developed and it has wide applications in the treatment of industrial effluents containing toxic pollutants, mainly heavy metals. The kinetics of the ion-exchange process involving Diphonix has not yet been investigated in such detail as in the present work. The models tested are useful for designing continuous fixed-bed column systems, were it is important to simulate the behavior of breakthrough curves. In the case of irreversible isotherms, the existence of very sharp concentration gradients in the column does not allow to get an efficient numerical solution of the model equations incorporating the PDM. The SCM, which takes into account non-steady diffusion, allows a better description of the problem and makes the numerical strategy more efficient for predicting the dynamics of the sorption process in column. As already mentioned in the introduction, the pseudo-steady state assumption has often been considered in shrinking-core type models and its application in order to correctly interpret the propagation of concentration waves in column is not appropriate. For sorption systems, the few studies reported in the literature on the SCM including the effect the transient diffusion were applied to regeneration of adsorbents [28,29].

5. Conclusions

The uptake of Cr(III) and Cu(II) by Diphonix resin from aqueous solutions was investigated. The methodology involved the determination of individual ion-exchange equilibrium isotherms for each pair metal/resin and kinetic experiments for Cr(III). The equilibrium isotherms as almost irreversible and were well fitted with the Langmuir–Freundlich and Langmuir models. From this analysis, the maximum exchange capacity at $T = 25\,^{\circ}C$ determined for Cr(III) was 2.73 meq/$g_{dryresin}$, and for Cu(II) was 2.45 meq/$g_{dryresin}$. The exchange capacity increased with increase in temperature due probably to the formation of more stable chelates between the metal ions and the functional groups of the resin. Moreover, the sorption capacity is also affected when the HNO_3 concentration present in the solutions is varied.

Regarding the kinetics of uptake of Cr(III), the pseudo-second-order kinetic model was found to fit very well the experimental data. The kinetic mechanism of the sorption of the metal into Diphonix is controlled by the intraparticle diffusion and was analyzed by the pore diffusion and shrinking core models. Both models described very well the evolution of chromium concentration in the external solution with time. The concentration of the sodium released by the resin varying along the time was only predicted by the shrinking core model. This model revealed to be more suitable for interpreting the kinetic process taking into account the irreversible character of the sorption of Cr(III) by the resin. The fitting of the model equations to the kinetic data enabled to determinate the effective pore diffusivity for Cr(III), i.e. $D_{pef} = 2.66–5.31 \times 10^{-11}$ m^2/s. This transport parameter was influenced by the chromium initial concentration. The SCM seems to be suitable for simulating the ion-exchange processes in fixed-bed directed to the treatment of industrial effluents containing heavy metals.

Acknowledgement

We would like to thank FCT (Foundation for Technology and Science) for its financial support for this work (Project POCTI/EQU/58149/2004).

References

[1] A.G. Chmielewski, T.S. Urbaĭnski, W. Migdal, Separation technologies for metals recovery from industrial wastes, Hydrometallurgy 295 (1997) 333–344.
[2] N. Kabay, M. Demircioğlu, H. Ekinci, M. Yŭksel, M. Sağlam, M. Akçay, M. Streat, Removal of metal pollutants (Cd(II) and Cr(III)) from phosphonic acid solutions by chelating resins containing phosphonic or diphosphonic groups, Ind. Eng. Chem. Res. 37 (1998) 2541–2547.
[3] S. Yalçin, R. Apak, J. Hizal, H. Afşar, Recovery of copper (II) and chromium (III,VI) from electro-plating industry wastewater by ion exchange, Sep. Sci. Technol. 36 (2001) 2181–2196.
[4] S.H. Lin, C.D. Kiang, Chromic acid recovery from waste acid solution by an ion exchange process: equilibrium and column ion exchange modelling, Chem. Eng. J. 92 (2003) 193–199.
[5] F. Gode, E. Pehlivan, A comparative study of two chelating ion-exchange resins for the removal of chromium (III) from aqueous solution, J. Hazard. Mater. B100 (2003) 231–243.
[6] S. Kocaoba, G. Akcin, Removal of chromium (III) and cadmium (II) from aqueous solutions, Desalination 180 (2005) 151–156.
[7] R.-S. Juang, H.-C. Kao, W. Chen, Column removal of Ni(II) from synthetic electroplating waste water using a strong-acid resin, Sep. Purif. Technol. 49 (2006) 36–42.
[8] F.C. Gazola, M.R. Pereira, M.A.S.D. Barros, E.A. Silva, P.A. Arroyo, Removal of Cr^{+3} in fixed bed using zeolite NaY, Chem. Eng. J. 117 (2006) 253–261.
[9] R. Chiarizia, E.P. Horwitz, S.D. Alexandratos, A.Q. Trochimczuk, D.W. Crick, Uptake of metal ions by a new chelating ion exchange resin. Part 2. Acid dependencies of transition and post-transition metal ions, Solvent Extr. Ion Exch. 11 (1994) 967–985.
[10] R. Chiarizia, E.P. Horwitz, S.D. Alexandratos, Uptake of metal ions by a new chelating ion-exchange resin. Part 4. Kinetics, Solvent Extr. Ion Exch. 12 (1994) 211–237.
[11] Y. Ho, G. McKay, Kinetic models for the sorption of dye from aqueous solution by wood, Process Saf. Environ. Protect. 76 (1998) 183–191.
[12] Y.S. Ho, G. McKay, Pseudo-second order model for sorption processes, Process Biochem. 34 (1999) 451–465.
[13] S. Rengaraj, C.K. Joo, Y. Kim, J. Yi, Kinetics of removal of chromium from water and electronic process wastewater by ion exchange resins: 1200H, 1500H and IRN97H, J. Hazard. Mater. B102 (2003) 257–275.
[14] Y. Ho, Review of second-order models for adsorption systems, J. Hazard. Mater. B136 (2006) 681–689.
[15] M. Dinesh, K.P. Singh, V.K. Singh, Trivalent chromium removal from wastewater using low cost activated carbon derived from agricultural waste material and activated carbon fabric cloth, J. Hazard. Mater. 135 (2006) 280–295.
[16] A. Sar, M. Tuzen, Kinetic and equilibrium studies of biosorption of Pb(II) and Cd(II) from aqueous solution by macrofungus (*Amanita rubescens*) biomass, J. Hazard. Mater. 164 (2009) 1004–1011.
[17] A. Fernández, M. Diaz, A. Rodrigues, Kinetic mechanisms in ion exchange processes, Chem. Eng. J. 57 (1995) 17–25.
[18] E. Arévalo, M. Rendueles, A. Fernández, A. Rodrigues, M. Diáz, Uptake of copper and cobalt in a complexing resin: shrinking core model with two reaction fronts, Sep. Purif. Technol. 13 (1998) 37–46.
[19] G.W. Dicinoski, L.R. Gahan, P.J. Lawson, J.A. Rideout, Application of the shrinking core model to the kinetics of extraction of gold(I), silver(I) and nickel(II) cyanide complexes by novel anion exchange resins, Hydrometallurgy 56 (2000) 323–336.
[20] M. Pritzker, Shrinking core model for multispecies uptake onto an ion exchange resin involving distinct reaction fronts, Sep. Purif. Technol. 42 (2005) 15–24.
[21] N.K. Madsen, R.F. Sincovec, Pdecol, general collocation software for partial differential equations, ACM Trans. Math. Software 5 (1979) 326–351.
[22] J. Villadsen, M.L. Michelsen, Solution of Differential Equations by Polynomial Approximation, Prentice-Hall, New York, 1978.

[23] LSODE, LSODI, ACM Signum News Lett. 15 (1980) 10.
[24] W.E. Stewart, M. Caracotsios, J.P. SZrensen, Software Documentation of GREG-General Regression Software Package for Nonlinear Parameter Estimation, University of Wisconsin-Madison, Madison, WI, 1993.
[25] S.A. Cavaco, S. Fernandes, C.M. Augusto, M.J. Quina, L.M. Gando_Ferreira, Evaluation of chelating ion-exchange resins for separating Cr(III) from industrial effluents, J. Hazard. Mater. 169 (2009) 516–523.
[26] S. Fernandes, Master Thesis, University of Coimbra, 2007.
[27] F. Gode, Removal of chromium ions from aqueous solutions by the adsorption method, in: A.A. Lewinsky (Ed.), Hazardous Materials and Wastewater: Treatment, Removal and Analysis, Nova Science Publishers, Inc., New York, 2007, pp. 275–308.
[28] A.M Ramos, M. Otero, A.E. Rodrigues, Recovery of vitamin B12 and cephalosporin-C from aqueous solutions by adsorption on non-ionic polymeric adsorbents, Sep. Purif. Technol. 38 (2004) 85–98.
[29] C. Costa, A. Rodrigues, Regeneration of polymeric adsorbents in a CSTR, Chem. Eng. Sci. 40 (1985) 707–713.